

229  
GL03536

## Vertical Gradients of Heat Production in the Continental Crust

### 2. Some Estimates from Borehole Data

ARTHUR H. LACHENBRUCH

*U.S. Geological Survey, Menlo Park, California 94025*

CARL M. BUNKER

*U.S. Geological Survey, Denver, Colorado 80225*

Vertical gradients of heat production were estimated from measurements on samples from eight boreholes in granitic rocks. Samples contained from 10 to 100 specimens, and the borehole depths range from 350 meters to 3 km. For holes less than 1 km deep the scatter of results is consistent with theoretical expectations based on known small-scale inhomogeneities. Gradient estimates from the deeper holes are not strongly influenced by such inhomogeneities, but their uncertainty cannot be evaluated statistically because of the possible effects of small perturbations of longer wavelength. The data suggest a general decrease in heat production with depth in the granitic rocks of a magnitude consistent with the exponential source model, although alternate models are not precluded. A 3-km hole in schist did not exhibit this trend, consistent with the view that upward concentration of sources occurred in the presence of a melted phase. As uncertainties in the numerical results are large and difficult to evaluate, many more analyses will be needed to establish vertical heat-production trends with confidence.

The principal reason for surprise at the discovery of the linear heat-flow relation (discussed in the companion paper [Lachenbruch, 1971]) is that it implies that the heat flow from the earth's interior is indicated by the radioactivity of the rock that happens to be exposed today at the surface of a pluton. It is all the more surprising when it is considered that in establishing this relation no great care was taken in sampling these rocks; with a few notable exceptions, little attention was given to petrologic variations and other local geologic conditions. Clearly the relation cannot be true in detail, and the sampling problem requires further attention [see e.g., Rogers, 1964]. Nevertheless, the observability of this relation from results obtained to date, suggests that in some provinces at least, local geologic variations (over distances of a few kilometers) can be treated as effects of higher order.

It has been shown in the companion paper that determination of the near-surface vertical gradient of heat production taken with the linear heat-flow relation could, ideally, help determine

the form of the crustal heat-production curve. It has also been shown that departures from an ideal distribution small enough to permit the linear heat-flow relation might still be so large as to preclude meaningful estimates of the vertical gradient of heat production from measurements in boreholes. Nevertheless, several sets of such measurements were available from previous studies, and a few additional ones were obtained to examine this question empirically. In keeping with the implications of the linear heat-flow relation, implausible as they may seem, samples were generally selected without regard for the detailed petrologic information that was available from some holes. Extreme values were rejected on the basis of an arbitrary statistical criterion. (In most cases, however, these values could not have been anticipated by macroscopic examination of the specimen.) In general, geological details were not considered, and trends of heat production that might have been associated with them were therefore treated as perturbations. These measurements will be described and discussed in terms of the theory presented in the companion paper.

Specime  
equally s  
number of  
ble 1). T  
potassium  
each spec  
units of  
Birch, 195

A = 0.3

where U  
in per ce  
Those sa  
(‘uc,’ Ta  
spectrum  
Smith [I  
oratory.  
drill cutt  
lyzed in  
by the  
Bush [I  
technique  
DDB-H  
in the U  
page E2  
[1969])  
used in  
reference  
ter caus  
ably sub  
ter of he  
scale. It  
small-sc  
variatio  
unimpor

The s  
were tal  
the Sic  
Smith,  
sents a  
analyze  
a gra  
provin  
hole in  
and G  
DW-B  
metam  
[Ebens

Continental Crust  
Data

94025

80225

measurements on samples from 100 specimens, and the borehole 1 km deep the scatter of small-scale inhomogeneities, caused by such inhomogeneities, and the possible effects of small decrease in heat production. The exponential source model, which did not exhibit this trend, occurred in the presence of a large and difficult to evaluate, production trends with confi-

crustal heat-production curve. It is shown that departures from an exponential relation might still be so large that meaningful estimates of the vertical heat production from measurements. Nevertheless, several sets of measurements were available from previous boreholes. New additional ones were obtained to question empirically. In keeping with the assumptions of the linear heat-flow model as they may seem, samples were selected without regard for the information that was available from boreholes. Extreme values were re-analyzed as an arbitrary statistical test cases, however, these values were anticipated by macroscopic measurements of the specimen.) In general, geologic trends of heat production that might have been associated with the theory presented in the

SAMPLES AND HEAT-PRODUCTION MEASUREMENTS

Specimens were taken at approximately equally spaced depth intervals throughout a number of holes in western North America (Table 1). The uranium (U), thorium (Th), and potassium (K) contents were determined for each specimen, and the heat production  $A$ , in units of  $10^{-13}$  cal/cm<sup>3</sup> sec, was calculated [see Birch, 1954] from

$$A = 0.317\rho(0.73 U + 0.20 Th + 0.27 K) \quad (1)$$

where  $U$  and  $Th$  are expressed in ppm and  $K$  in per cent, and  $\rho$  is rock density in g/cm<sup>3</sup>. Those samples in the form of uncrushed core ('uc,' Table 1) were analyzed by gamma ray spectrometric techniques by Wollenberg and Smith [1964] at the Lawrence Radiation Laboratory. Those in the form of crushed core and drill cuttings ('cc' and 'dc,' Table 1) were analyzed in the U.S. Geological Survey laboratory by the gamma ray technique of Bunker and Bush [1966]. (An updated discussion of their technique is in preparation.) The sample from DDB-H-3 was analyzed by chemical methods in the U.S. Geological Survey laboratory (see page E2 and Table 14, Tilling and Gottfried [1969]). Details of the equipment and methods used in these laboratories can be found in the references cited. For most of the data, the scatter caused by errors in reproducibility is probably substantially smaller than the natural scatter of heat-production values on the hand-sample scale. In any case, the statistical measures of variations, and the distinction between them is unimportant in the present application.

The samples designated ST, SJ, JB, and HC were taken from core holes in granitic rocks of the Sierra Nevada batholith [Wollenberg and Smith, 1968; Lachenbruch, 1968]. HC-B represents a larger sample from the borehole HC, analyzed in a different laboratory. UE-1 is from a granitic pluton in the Basin and Range province, Nevada, and DDB-H-3 is from a core hole in the Boulder batholith, Montana [Tilling and Gottfried, 1969]. The samples DW and DW-B are from a deep hole in Precambrian metamorphic granitic rock in eastern Wyoming [Ebens and Smithson, 1966]. DW represents

TABLE 1. Heat Production Measurements

Sample	Form	L, km	No. Specimens	Heat Production			Uranium			Thorium			Potassium			Contribution to $A_m$ , per cent				
				$A_m$ , $10^{-13}$ cal $cm^{-3}$ $sec^{-1}$	$\sigma^*$ $A_m$	No. Rejected	$U_m$ , ppm	$\sigma^*$ $U_m$	No. Rejected	$Th_m$ , ppm	$\sigma^*$ $Th_m$	No. Rejected	$K_m$ , ppm	$\sigma^*$ $K_m$	No. Rejected	U	Th	K		
ST	uc	0.35	18	0.7	0.13	0	0.56	0.25	0	1.49	0.17	0	0.50	0.10	2	2.7	0.89	49	35	16
SJ	uc	0.46	15	2.2	0.23	2	1.99	0.30	1	3.92	0.15	2	1.31	0.11	2	2.0	0.66	55	29	16
JB	uc	0.49	17	3.5	0.18	1	2.97	0.18	0	6.73	0.28	1	1.61	0.15	1	2.3	0.54	55	34	11
HC	uc	0.55	19	8.9	0.13	1	7.74	0.23	0	21.1	0.10	1	2.99	0.04	1	2.7	0.39	53	40	7
HC-B	cc	0.55	109	9.1	0.17	6	7.99	0.24	2	20.8	0.18	4	3.14	0.06	2	2.6	0.39	54	38	8
UE-1	cc	0.51	60	4.2	0.11	3	2.89	0.21	2	10.9	0.11	1	3.29	0.04	4	4.2	1.3	38	44	18
DDH-E-3	ca	0.98	19	8.6	0.18	1	6.07	0.31	0	22.5	0.14	1	3.48	0.05	2	3.7	0.57	44	45	11
DW-W	uc	3.0	10	5.5	0.22	2	2.25	0.27	1	21.0	0.38	1	2.68	0.21	0	9.3	1.2	25	65	10
DW	dc	3.0	99	4.3	0.23	3	1.70	0.35	2	14.5	0.32	1	2.99	0.14	5	8.5	1.8	25	58	17
DC	dc	3.0	100	2.1	0.22	1	1.98	0.25	1	2.75	0.29	0	1.56	0.12	5	1.4	0.79	59	23	18
DA	dc	3.0	94	4.9	0.21	5	2.88	0.28	1	13.9	0.20	5	2.23	0.22	1	4.8	0.77	38	50	12

<sup>1</sup> uc, uncrushed core,  $\gamma$  ray, Lawrence Radiation Laboratory; cc, crushed core,  $\gamma$  ray, U. S. Geological Survey; ca, chemical analysis of core, U. S. Geological Survey; dc, drill cuttings,  $\gamma$  ray, U. S. Geological Survey.

ten samples of solid core analyzed by H. A. Wollenberg and A. R. Smith (unpublished data), and DW-B represents 99 samples of drill cuttings from the same hole analyzed in the U.S. Geological Survey laboratory. DC is a 3-km hole in Precambrian plutonic rock of the Canadian shield near Flin Flon, Manitoba (D. C. Findlay, unpublished data, 1966), and DA is a 3-km hole in schist near Fairbanks, Alaska (R. B. Forbes and F. R. Weber, unpublished data). Samples from both of these holes (DC and DA) were drill cuttings analyzed in the U.S. Geological Survey laboratory.

#### ANALYSIS OF DATA

For each of the eleven sets of data (Table 1) a regression line was passed through  $(\ln A, z)$  to determine the mean heat production  $A_m^*$ , its standard deviation  $\sigma^*$ , and the normalized gradient  $G^*$  and its standard error  $\gamma^*$ . These symbols are defined mathematically in the companion paper [Lachenbruch, 1971], where it is shown that if the only perturbations of  $A(z)$  (from the idealized distribution  $\phi(z)$ ) are random ones distributed log normally, these quantities represent reasonable estimates of means and variations for the quantities sought.

By a similar procedure, regression lines were determined individually for U, Th, and K for each set of data and the corresponding parameters determined.

The slope of a regression line is very sensitive to extreme values, improbable in a normal distribution, if these values occur near the ends of the depth interval. It is desirable to attempt to identify such points by applying some consistent, though arbitrary, criterion of rejection. For this purpose we adopted Chauvenet's criterion [see Misener *et al.*, 1951], wherein a value is rejected in a set of  $n$  measurements if it does not lie within the probability zone,  $1 - (1/2n)$ , for an  $n$ -member sample taken from a normal population  $Y(z_i)$ ,  $i = 1, 2, 3, \dots, n$ . Thus for  $n = 10$  we reject those values  $Y_i$  for which

$$Y_m^* |\ln Y(z_i) - \ln y(z_i)| > 1.96\sigma^* \quad (2)$$

where  $Y(z_i)$  and  $y(z_i)$  are the observed value and the value given by the regression line, respectively, at depth  $z_i$ , and  $Y_m^*$  is the geometric mean of  $Y_i$ . For  $n = 100$ , the numerical coefficient is 2.81. No theoretical significance is implied for the criterion in this application. It

is simply a convenient scheme for establishing the cutoff point for extreme values: about two standard deviations for the smallest samples up to almost three for the largest ones.

The means ( $A_m^*$ ,  $Th_m^*$ ,  $U_m^*$ ,  $K_m^*$ ), and standard deviations ( $\sigma^*$ ) obtained from each of these analyses are tabulated in Table 1. Element ratios and the relative contribution of individual elements to heat production are also tabulated. Among these samples the mean element concentrations and the ratio  $Th_m^*/U_m^*$  vary by an order of magnitude. Nevertheless, in all samples at least 80 to 90% of the heat production is accounted for by the U plus Th. Hence in analyzing  $A$ , the rejection of extreme values was applied only to U and Th; those depths at which either U or Th failed to satisfy the rejection criterion were deleted in the final linear regression analysis of  $(\ln A, z)$ .

In each of the holes, HC and DW, two independent samples were studied. It is seen that the 19 specimens of uncrushed core (HC) analyzed by Wollenberg and Smith yielded means for heat production, the individual element concentrations, and element ratios within a few per cent of those obtained from 109 specimens of crushed core (HC-B) independently sampled and analyzed by Bunker and Bush (Table 1). By contrast, the means for the two samples (DW and DW-W) from Wyoming, analyzed by the same two laboratories, differ by 30% or so. In this hole the uncrushed core sample (DW-W) was smaller (only 10 specimens), the rocks were more heterogeneous on both small and large scales, and the sample analyzed by Bunker and Bush (DW) was drill cuttings, not crushed core. When viewed statistically this discrepancy is significant, and it is not known which of the above factors is responsible for it. Although it is reassuring that both samples recovered the anomalous thorium-uranium ratio (9.3 for DW-W, 8.5 for DW), this matter deserves further study.

In Figure 1 the normalized gradient of heat production  $G^*$  is plotted against its standard error  $\gamma^*$  for each sample. The open circles represent results of the regression analysis for granitic rocks with all depths included, and the solid circles represent results after extreme values were rejected. The horizontal distance between the dashed curves represents a band of width  $2\gamma^*$ . The curves are arbitrarily drawn

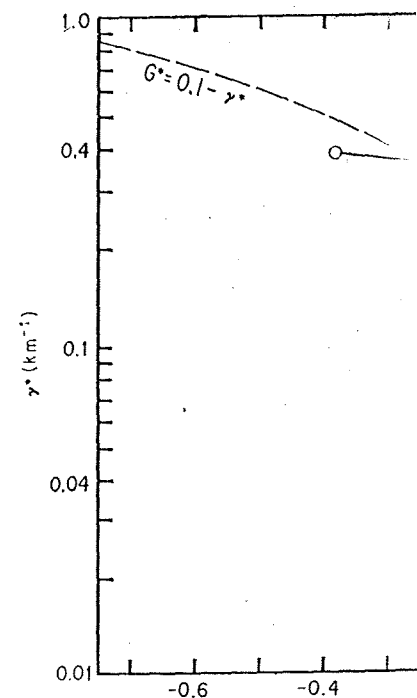


Fig. 1. Mean normalized gradient from regression analysis of samples; all data in each sample; closed circles represent samples from which extreme values were rejected; open circles represent the weighted mean of all samples in the region  $G^* = 0.1 \pm \gamma^*$ . Information from Lachenbruch [1971].

centered at the value  $G^* = 0.1$  km<sup>-1</sup>. If there were a universal gradient  $G^*$  to all the localities represented, if its value were  $0.1$  km<sup>-1</sup>, and if the only departures from such a gradient were small-scale ones with a lognormal distribution, the point of Figure 1 would have a 68% probability of lying between the dashed curves.

Points lying to the right of  $G^* = 0.1$  represent heat production decreasing with depth; those to the left indicate an increase in heat production with depth. It is shown (Table 1, Lachenbruch [1971]) that simple decreasing source models imply a linear heat-flow relation lead to  $G^* = 0.1$  km<sup>-1</sup>. Except for the three large sam-

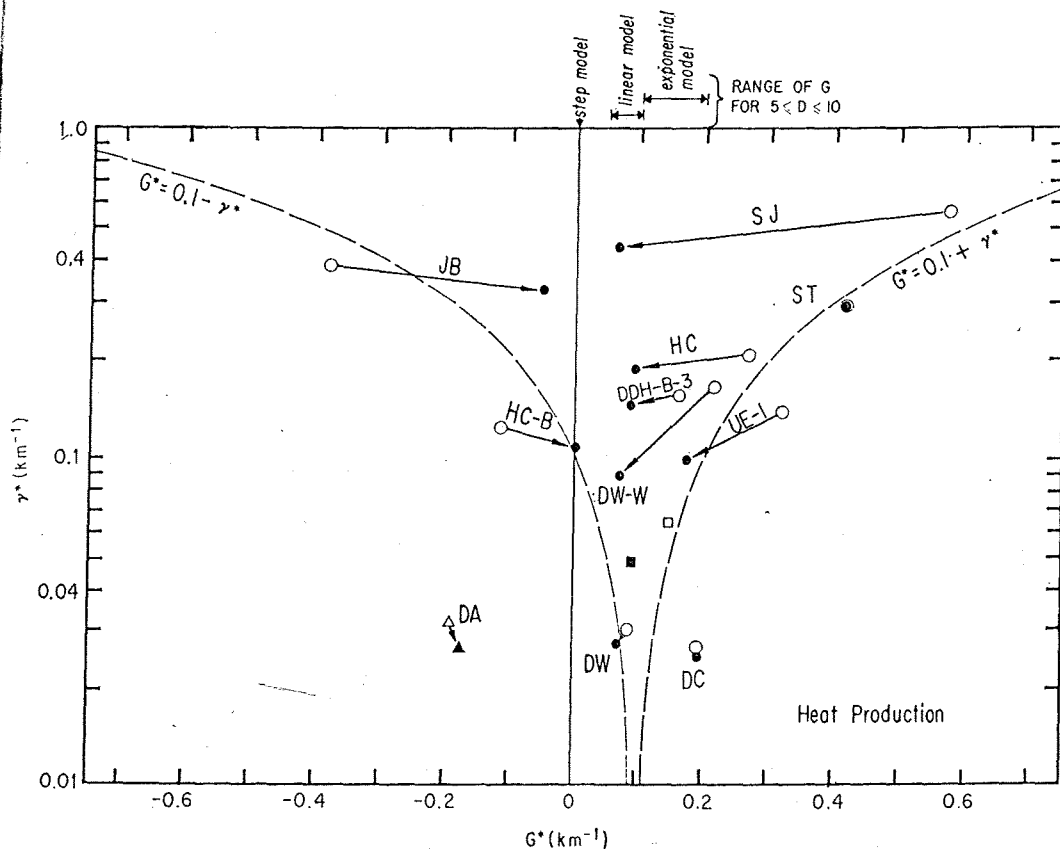


Fig. 1. Mean normalized gradient  $G^*$  of heat production and its standard error  $\gamma^*$  obtained from regression analysis of samples described in Table 1. Open symbols represent results from all data in each sample; closed symbols represent results after extreme values were rejected. Circles represent samples from granitic rock; triangle represents sample from schist. Squares represent the weighted mean of all samples except DA, DW, and DC. Dashed curves bound the region  $G^* = 0.1 \pm \gamma^*$ . Information in upper margin summarizes Table 1 of *Lachenbruch* [1971].

centered at the value  $G^* = 0.1 \text{ km}^{-1}$ . Thus if there were a universal gradient  $G(\phi)$  common to all the localities represented, if its value were  $0.1 \text{ km}^{-1}$ , and if the only departures from a line with such a gradient were small-scale random ones with a lognormal distribution, then each point of Figure 1 would have a 68% probability of lying between the dashed curves.

Points lying to the right of  $G^* = 0$  (Figure 1) represent heat production decreasing with depth; those to the left indicate an increase in heat production with depth. It has been shown (Table 1, *Lachenbruch* [1971]) that simple decreasing source models implied by the linear heat-flow relation lead to  $G(\phi) \sim 0.1 \text{ km}^{-1}$ . Except for the three large samples from

deep holes (DA, DW, DC), the standard error ( $\gamma^*$ ) equals or exceeds that value (Figure 1), and little significance can be attached even to the sign of individual values of  $G^*$  determined from them. It is seen that for these particular data there seems to be a tendency toward positive  $G^*$ , and the question arises whether these large-uncertainty values have some collective statistical significance. As the spread in  $G^*$  is of the order of  $\gamma^*$ , it might be assumed without inconsistency that each data set is associated with the same value of  $G(\phi)$  and the only departures are random small-scale ones. They could then be identified with a weighted mean  $G_m$  and its standard error  $\gamma(G_m)$  as follows [*Topping*, 1957, p. 87]:

... a convenient scheme for establishing a point for extreme values: about two deviations for the smallest samples up to three for the largest ones. Means ( $A_m^*$ ,  $Th_m^*$ ,  $U_m^*$ ,  $K_m^*$ ), and deviations ( $\sigma^*$ ) obtained from each analysis are tabulated in Table 1. Ratios and the relative contribution of elements to heat production are also given. Among these samples the mean element concentrations and the ratio  $Th_m^*/U_m^*$  are of order of magnitude. Nevertheless, at least 80 to 90% of the heat production is accounted for by the U plus Th. In analyzing A, the rejection of extreme values was applied only to U and Th; those which either U or Th failed to satisfy the criterion were deleted in the final regression analysis of  $(\ln A, z)$ . Of the holes, HC and DW, two in which samples were studied. It is seen that means of uncrushed core (HC) analyses by Lachenbruch and Smith yielded means of heat production, the individual element concentrations and element ratios within a few per cent of those obtained from 109 specimens of uncrushed core (HC-B) independently sampled by Bunker and Bush (Table 1). The means for the two samples analyzed by DW-W from Wyoming, analyzed by two laboratories, differ by 30% or so. In the uncrushed core sample (DW-W) from only 10 specimens, the rocks were heterogeneous on both small and large scales. The sample analyzed by Bunker and Bush was drill cuttings, not crushed. Reviewed statistically this discrepancy was found and it is not known which of the two is responsible for it. Although it is noted that both samples recovered the same thorium-uranium ratio (9.3 for DW), this matter deserves fur-

... the normalized gradient of heat production is plotted against its standard error for each sample. The open circles represent results from regression analysis for all depths included, and the closed circles represent results after extreme values were rejected. The horizontal distance between the dashed curves represents a band of uncertainty. The curves are arbitrarily drawn

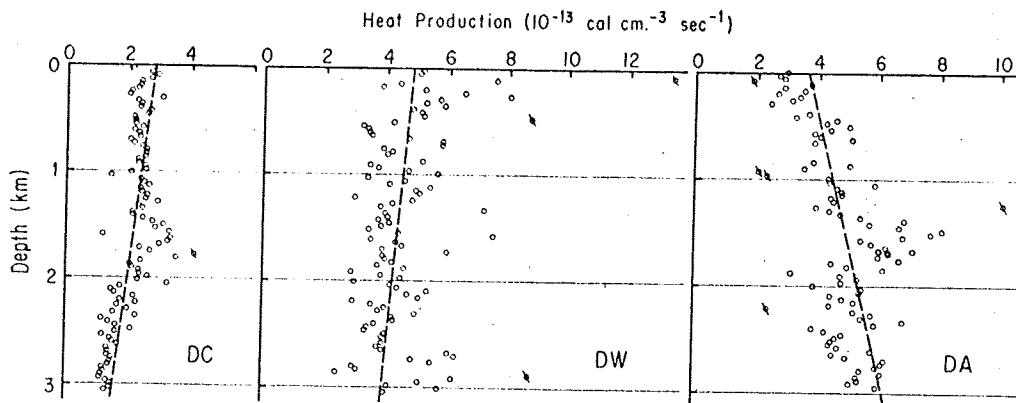


Fig. 2. Heat production of samples from two deep boreholes in granitic rock (DC and DW) and one in schist (DA). Circles with diagonal lines represent points rejected by the analysis. Regression line is dashed.

$$G_m = \frac{\sum_{i=1}^p \left( \frac{G_i^*}{\gamma_i^{*2}} \right)}{\sum_{i=1}^p \frac{1}{\gamma_i^{*2}}} \quad (3)$$

$$\gamma(G_m) = \left[ \frac{\sum_{i=1}^p \frac{(G - G_i^*)^2}{\gamma_i^{*2}}}{(p-1) \sum_{i=1}^p \frac{1}{\gamma_i^{*2}}} \right]^{1/2}$$

where  $p$  is the number of data pairs ( $G^*$ ,  $\gamma^*$ ), in this case 8. The values of  $G_m$ ,  $\gamma(G_m)$  for the

data with no points rejected are shown as an open square (Figure 1), and the corresponding values for the data without extreme values are shown as the solid square. Their significance is discussed in the next section.

The values of  $G^*$  for the three deep holes (Figure 1) differ from one another by several standard errors ( $\gamma^*$ ) when interpreted in terms

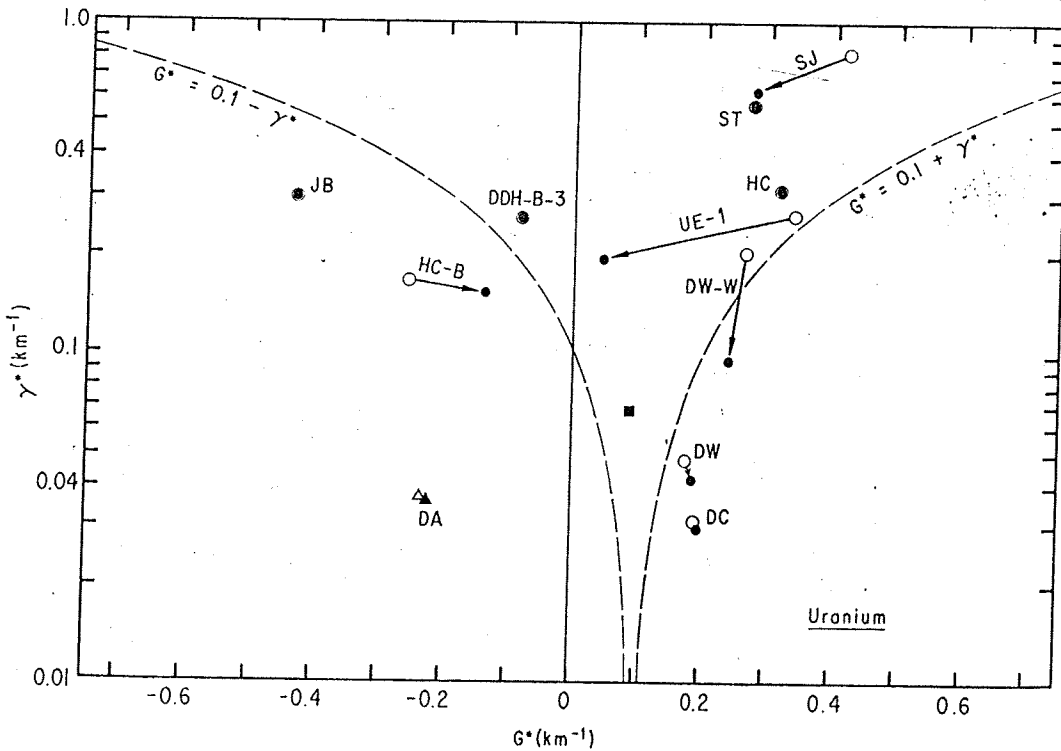


Fig. 3. Data for uranium presented in the format of Figure 1.

of the assumptions that  $G(\phi)$  is the both sites and that the only departures are random small-scale ones. However, DC and DA show decreasing heat production with depth of the order of magnitude suggested by the models in Table 1. The difference between them could be explained, for example, by a systematic departure from  $\phi$  with a  $v$  equal to the hole depth (3 km) and an amplitude of 10 or 15%  $A_m^*$  (Fig. 4, Lachenbruch [1971]).

The third deep hole DA, which is the only one that shows a significant trend in heat production with depth ( $G^* = \gamma^* \approx 0.026$ ). It is discussed further in the next section.

In Figure 2, heat production is shown as a function of depth for the three deep boreholes. In addition to small-scale random fluctuations, long-wavelength perturbations are evident in the DA hole. As anticipated in the previous section [Lachenbruch, 1971], when these perturbations are viewed 1 km at a time, the 3-km trend does not generally appear. Whether or not this trend is generally significant, of course, depends on unknown departures of greater

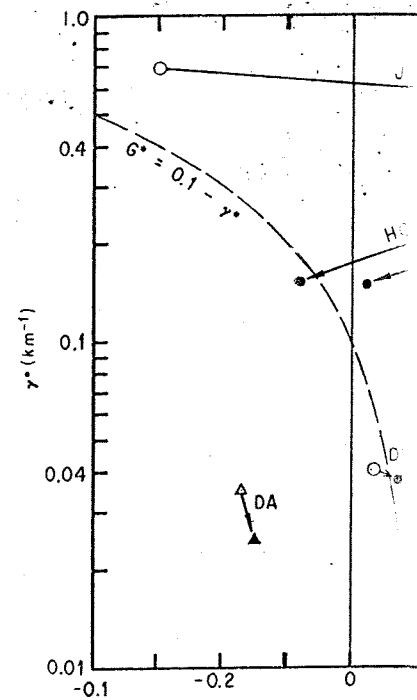
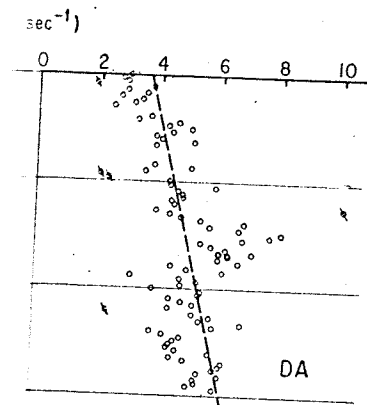


Fig. 4. Data for



es in granitic rock (DC and present points rejected by the

points rejected are shown as an Figure 1), and the correspond the data without extreme values the solid square. Their significance the next section.

of  $G^*$  for the three deep holes from one another by several ( $\gamma^*$ ) when interpreted in terms

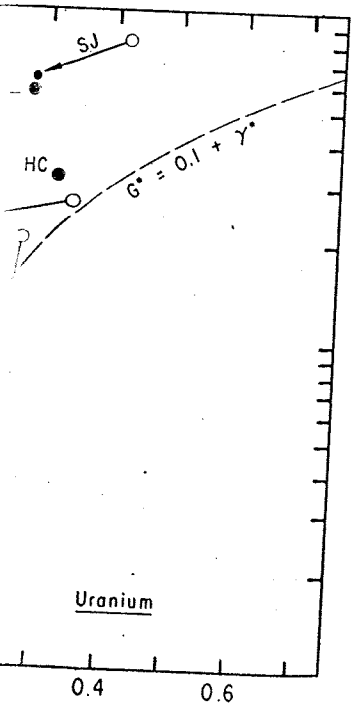


Figure 1.

of the assumptions that  $G(\phi)$  is the same at both sites and that the only departures are random small-scale ones. However, both DW and DC show decreasing heat production with depth of the order of magnitude suggested by the models in Table 1. The difference between them could be explained, for example, by a systematic departure from  $\phi$  with a wavelength equal to the hole depth (3 km) and an amplitude of 10 or 15%  $A_m^*$  (Fig. 4, *Lachenbruch* [1971]).

The third deep hole DA, which is in schist, is the only one that shows a significant increase in heat production with depth ( $G^* \approx -0.175$ ,  $\gamma^* \approx 0.026$ ). It is discussed further below.

In Figure 2, heat production is shown as a function of depth for the three deep holes. In addition to small-scale random fluctuations, longer wavelength perturbations are evident in each hole. As anticipated in the previous discussion [*Lachenbruch*, 1971], when these graphs are viewed 1 km at a time, the 3-km trend does not generally appear. Whether or not the 3-km trend is generally significant, of course, depends on unknown departures of greater wavelength.

Although trends in heat production are important in geothermal studies, they are less fundamental from a geochemical point of view than trends in the distribution of individual heat-producing elements. In Figures 3 and 4 the individual data for U and Th are presented in the same form as Figure 1. As might be expected the trend toward a decrease with depth for granitic rocks is indicated in both of these plots. The strong tendency toward an increase with depth is shown individually for U and Th in the hole in schist (DA). For the shallower holes the scatter in  $G^*$  is somewhat greater for U and Th individually than for A, as one might expect when two random samples are combined, thereby effectively increasing the sample size and decreasing the standard error.

The plot for potassium, which has only a minor effect on heat production, is shown as Figure 5. It is seen that the differences between the values of  $G^*$  are large relative to  $\gamma^*$  and indicate systematic departures from a simple hypothetical curve, not attributable to random small-scale variations. However, even

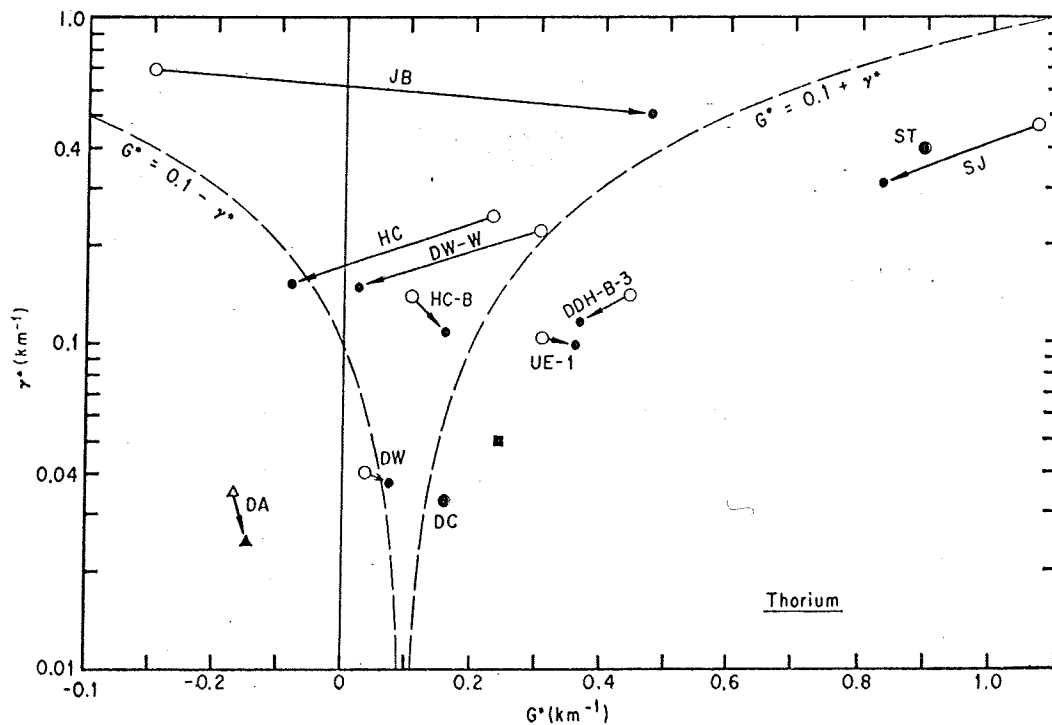


Fig. 4. Data for thorium presented in the format of Figure 1.

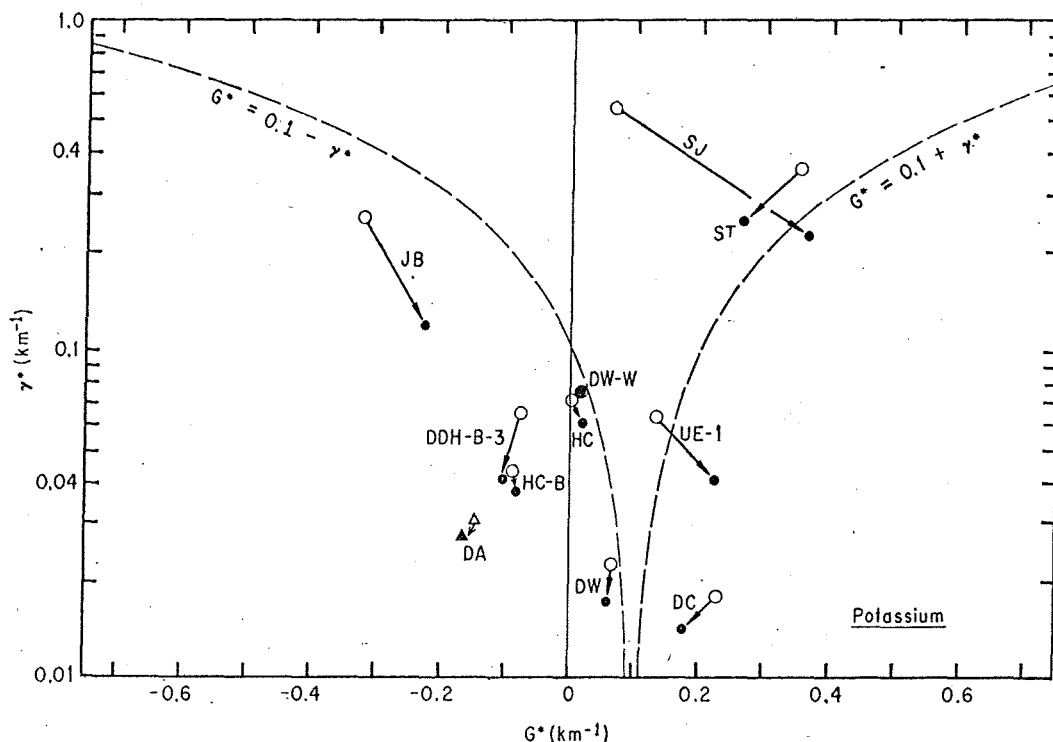


Fig. 5. Data for potassium presented in the format of Figure 1.

for potassium, the deepest holes in granite suggest a positive value of  $G^*$ .

DISCUSSION

Numerical summaries of the data on vertical gradients of heat production are given in Table 2. The first line represents the open and solid squares of Figure 1, a mean of the 8 high-uncertainty estimates of  $G^*$  with each value weighted by the reciprocal of the square of  $\gamma^*$ . This averaging procedure could be justified if it were known that (1)  $G(\phi)$  had the same value

at each of the 7 locations represented by these 8 samples, and (2) departures from this value were only small-scale, random ones. The first of these conditions may be nearly fulfilled as 6 of the 7 locations yield ( $q, A$ ) values that lie very close to the Sierra or Basin and Range curves, both of which yield a value of  $D$  of about 10 km [Roy et al., 1968; Lachenbruch, 1968]. The remaining (and most heavily weighted) sample DW-W, is associated with a ( $q, A$ ) value closer to the 'stable continental' curve for which  $D$  might be somewhat less. However, this difference

TABLE 2. Numerical Summary of Data

	All Data				Extreme Values Rejected			
	(1) $G^*$	(2) $\gamma^*$	(3) $(G^*)^{-1}$	(4) $(G^* \pm \gamma^*)^{-1}$	(5) $G^*$	(6) $\gamma^*$	(7) $(G^*)^{-1}$	(8) $(G^* \pm \gamma^*)^{-1}$
Weighted mean of (8) (excludes DC, DW, DA)	0.14	0.07	7.3	4.8-14.2	0.09	0.05	11.3	7-25
DC	0.190	0.026	5.26	4.6-6.1	0.192	0.025	5.20	4.6-6
DW	0.082	0.030	12.2	8.9-19.2	0.068	0.027	14.7	10.5-24
1/2 (DC + DW)	0.136	...	7.4	...	0.130	...	7.7	...
DA (schist)	-0.189	0.032	-5.3	(-4.5)-(-6.4)	-0.174	0.026	-5.7	(-5.0)-(-6.8)

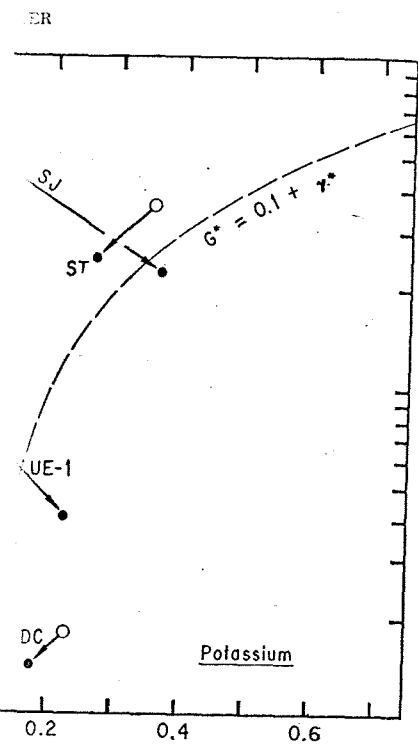
Unit of  $G^*$  and  $\gamma^*$  is km.

is small relative to the scatter in  $G^*$ . Insofar as the second condition is seen from Figure 1 that the could, indeed, be accounted for small-scale fluctuations alone. However, results for U and Th individually (4) are less convincing, and the need of unknown perturbations of longer render this averaging procedure suggestive. Thus it is surprising that value of  $(G^*)^{-1}$ , (7.3 km for all cleared data) is close to  $D$ , expected from the exponential model from columns 4 and 8, Table 2, even under the foregoing assumptions. Determinations are highly uncertain, the specific numerical agreement fortuitous, the sign and magnitude of results seem to favor source function increase with depth rather like the exponential models.

The value of  $(G^*)^{-1}$  for two holes from 3-km holes in granite are consistent with the results from the same just discussed. The difference in  $G^*$  between two holes ( $\sim 4\gamma^*$ ) is not likely to be principally from small-scale fluctuations. A different  $G(\phi)$  obtains at each of the 7 locations represented by these 8 samples, and (2) departures from this value were only small-scale, random ones. The first of these conditions may be nearly fulfilled as 6 of the 7 locations yield ( $q, A$ ) values that lie very close to the Sierra or Basin and Range curves, both of which yield a value of  $D$  of about 10 km [Roy et al., 1968; Lachenbruch, 1968]. The remaining (and most heavily weighted) sample DW-W, is associated with a ( $q, A$ ) value closer to the 'stable continental' curve for which  $D$  might be somewhat less. However, this difference is small relative to the scatter in  $G^*$ . Insofar as the second condition is seen from Figure 1 that the could, indeed, be accounted for small-scale fluctuations alone. However, results for U and Th individually (4) are less convincing, and the need of unknown perturbations of longer render this averaging procedure suggestive. Thus it is surprising that value of  $(G^*)^{-1}$ , (7.3 km for all cleared data) is close to  $D$ , expected from the exponential model from columns 4 and 8, Table 2, even under the foregoing assumptions. Determinations are highly uncertain, the specific numerical agreement fortuitous, the sign and magnitude of results seem to favor source function increase with depth rather like the exponential models.

The value of  $(G^*)^{-1}$  for two holes from 3-km holes in granite are consistent with the results from the same just discussed. The difference in  $G^*$  between two holes ( $\sim 4\gamma^*$ ) is not likely to be principally from small-scale fluctuations. A different  $G(\phi)$  obtains at each of the 7 locations represented by these 8 samples, and (2) departures from this value were only small-scale, random ones. The first of these conditions may be nearly fulfilled as 6 of the 7 locations yield ( $q, A$ ) values that lie very close to the Sierra or Basin and Range curves, both of which yield a value of  $D$  of about 10 km [Roy et al., 1968; Lachenbruch, 1968]. The remaining (and most heavily weighted) sample DW-W, is associated with a ( $q, A$ ) value closer to the 'stable continental' curve for which  $D$  might be somewhat less. However, this difference is small relative to the scatter in  $G^*$ . Insofar as the second condition is seen from Figure 1 that the could, indeed, be accounted for small-scale fluctuations alone. However, results for U and Th individually (4) are less convincing, and the need of unknown perturbations of longer render this averaging procedure suggestive. Thus it is surprising that value of  $(G^*)^{-1}$ , (7.3 km for all cleared data) is close to  $D$ , expected from the exponential model from columns 4 and 8, Table 2, even under the foregoing assumptions. Determinations are highly uncertain, the specific numerical agreement fortuitous, the sign and magnitude of results seem to favor source function increase with depth rather like the exponential models.

more observations of this kind from will be needed before trends of heat with depth can be established with It has been suggested [Lachenbruch] that heat sources are exponentially distributed in the crust in the presence of a magma during the evolution of granitic rocks. This view would not seem inconsistent with the model described above or with geochemical data [see e.g., Lambert and Heier, 1967]. A counter example is provided by



format of Figure 1.

the 7 locations represented by these 8 and (2) departures from this value small-scale random ones. The first of variations may be nearly fulfilled as 6 of ions yield ( $q, A$ ) values that lie very the Sierra or Basin and Range curves. which yield a value of  $D$  of about 10 [Lachenbruch, 1968; Lachenbruch, 1968]. The (and most heavily weighted) sample associated with a ( $q, A$ ) value closer 'stable continental' curve for which  $D$  somewhat less. However, this difference

Extreme Values Rejected			
(5)	(6)	(7)	(8)
$G^*$	$\gamma^*$	$(G^*)^{-1}$	$(G^* \pm \gamma^*)^{-1}$
0.09	0.05	11.3	7-25
0.192	0.025	5.20	4.6-6
0.068	0.027	14.7	10.5-24
0.130	...	7.7	...
0.174	0.026	-5.7	(-5.0) - (-6.8)

is small relative to the scatter in  $G^*$  (Figure 1). Insofar as the second condition is concerned, it is seen from Figure 1 that the scatter in  $G^*$  could, indeed, be accounted for by random small-scale fluctuations alone. However, the results for U and Th individually (Figures 3 and 4) are less convincing, and the neglected effects of unknown perturbations of longer wavelengths render this averaging procedure no more than suggestive. Thus it is surprising that the mean value of  $(G^*)^{-1}$ , (7.3 km for all data, 11.3 km for cleared data) is close to  $D$ , the value expected from the exponential model. However, from columns 4 and 8, Table 2, it is seen that even under the foregoing assumptions these determinations are highly uncertain. Although the specific numerical agreement is probably fortuitous, the sign and magnitude of the results seem to favor source functions that decrease with depth rather like the exponential or linear models.

The value of  $(G^*)^{-1}$  for two large samples from 3-km holes in granite are in the range from 5-15 km (columns 3 and 7, Table 2), consistent with the results from the smaller samples just discussed. The difference in  $G^*$  for these two holes ( $\sim 4\gamma^*$ ) is not likely to have resulted principally from small-scale fluctuations. Either a different  $G(\phi)$  obtains at each site or the difference results from longer wavelength perturbations. A simple average of the  $G^*$  values has a reciprocal of about  $7\frac{1}{2}$  km (Table 2). This is the value of  $D$  given by Roy *et al.* [1968] for 'stable' regions, the most probable province assignment for these stations. Once again these particular numerical values cannot be taken too seriously, but the results suggest heat production decreasing with depth at a rate comparable to that expected from the exponential model. Discrimination among similar decreasing source models is, of course, not possible, and many more observations of this kind from deep holes will be needed before trends of heat production with depth can be established with confidence.

It has been suggested [Lachenbruch, 1970] that heat sources are exponentially redistributed in the crust in the presence of a melted phase during the evolution of granitic rocks, and this view would not seem inconsistent with the data described above or with geochemical evidence [see e.g., Lambert and Heier, 1967]. A supporting counter example is provided by data from

DA, as it is the only sample that shows a significant increase in heat production with depth (Figure 2). It is also the only sample not taken from granitic rock. The material at this site, a schist, has never reached the minimum melting conditions according to detailed petrographic studies (R. B. Forbes and F. R. Weber, unpublished data; R. B. Forbes, oral communication).

*Acknowledgments.* Harold Wollenberg and Allan Smith of the University of California, Lawrence Radiation Laboratory, kindly permitted our use of their heat-production data for the sample 'DW-W.' We are grateful for comments on the manuscript by Francis Birch, Alfred Miesch, John Sass, W. H. K. Lee, and B. V. Marshall. Publication has been authorized by the Director, U.S. Geological Survey.

REFERENCES

Birch, Francis. Heat from radioactivity, in *Nuclear Geology*, edited by H. Paul, chap. 5, John Wiley, New York, 1954.

Bunker, C. M., and C. A. Bush, Uranium, thorium, and radium analyses by gamma-ray spectrometry (0.184-0.352 million electron volts), *U. S. Geol. Surv. Prof. Pap.* 550-B, B-176, 1966.

Ebens, R. J., and S. B. Smithson, Petrography of Precambrian rocks from a 3.05-kilometer-deep borehole, Wind River Mountains, Wyoming, *Contrib. Geol.*, 5, 31, 1966.

Lachenbruch, A. H., Preliminary geothermal model of the Sierra Nevada, *J. Geophys. Res.*, 73, 6977, 1968.

Lachenbruch, A. H., Crustal temperature and heat production: Implications of the linear heat-flow relation, *J. Geophys. Res.*, 75, 3291, 1970.

Lachenbruch, A. H., Vertical gradients of heat production in the continental crust, 1, Theoretical detectability from near-surface measurements, *J. Geophys. Res.*, 76, this issue, 1971.

Lambert, I. B., and K. S. Heier, The vertical distribution of uranium, thorium, and potassium in the continental crust, *Geochim. Cosmochim. Acta*, 31, 377, 1967.

Misener, A. D., L. G. D. Thompson, and R. J. Uffen, Terrestrial heat flow in Ontario and Quebec, *Trans. AGU*, 32, 729, 1951.

Rogers, J. J. W., Statistical tests of the homogeneity of the radioactive components of granitic rocks, in *The Natural Radiation Environment*, edited by J. A. S. Adams and W. M. Lowder, pp. 51-62, University of Chicago Press, 1964.

Roy, R. F., D. D. Blackwell, and Francis Birch, Heat generation of plutonic rocks and conti-



mental heat flow provinces, *Earth Planet. Sci. Lett.*, **5**, 1, 1968.

Tilling, R. I., and David Gottfried, Distribution of thorium, uranium, and potassium in igneous rocks of the Boulder batholith region, Montana, and its bearing on radiogenic heat production and heat flow, *U. S. Geol. Surv. Prof. Pap. 614-E*, 29 pp., 1969.

Topping, J., *Errors of Observation and Their Treatment*, 119 pp., Unwin Brothers, London, 1957.

Wollenberg, H. A., and A. R. Smith, Radioactivity and radiogenic heat in Sierra Nevada plutons, *J. Geophys. Res.*, **69**, 3471, 1964.

Wollenberg, H. A., and A. R. Smith, Radiogeologic studies in the central part of the Sierra Nevada batholith, California, *J. Geophys. Res.*, **73**, 1481, 1968.

(Received January 11, 1971;  
revised March 1, 1971.)

## Focal Mechanism of

Department  
Massachusetts Institute

Body and surface waves for a middle of the Nazca plate indicate axis in the east-west direction. The direction of plate motion. A focal mechanism determined from a combination of azimuthal radiation pattern forms characteristic can be used for analysis of the continental margin on surface energy without reflections or changes. Rayleigh waves by the continental margins due to the continental margin.

A simplified form of the ocean tectonics proposed in the theory of the newtonics [Isacks *et al.*, 1968], variants aside, consists of a rigid slab that generated in the ocean ridge dissects horizontally away from it and finally backward and sinks under the continental type margin.

Difficulties arise when one tries to determine the driving mechanism of this model. The most generally accepted driving mechanism is a convective current in the mantle [L. Hess, 1962], but other secondary mechanisms have been postulated, e.g., the pull of the sinking slab [Isacks *et al.*, 1969], and hydrostatic overpressure [Orwan, 1964]. Each mechanism must account for at least part of the observations, and none can be completely discarded. This situation arises from the possible complexity of the process, in which all those driving forces are present, but additional data would help to determine their relative importance.

The stresses in the slab, at the ridge and under the continent are presumably compressional [e.g., Sykes, 1967; Isacks and McMechen, 1969], but the stresses in the oceanic plate between ridge and continent have not been determined. Their determination